THE JOURNAL OF BIOLOGICAL CHEMISTRY VOL. 287, NO. 10, pp. 7374–7387, March 2, 2012

Different Modalities of Intercellular Membrane Exchanges Mediate Cell-to-cell P-glycoprotein Transfers in MCF-7 Breast Cancer Cells*[S]

Received for publication, October 12, 2011, and in revised form, December 13, 2011 Published, JBC Papers in Press, January 6, 2012, DOI 10.1074/jbc.M111.312157

Jennifer Pasquier[‡§1], Ludovic Galas[§], Céline Boulangé-Lecomte[‡], Damien Rioult[‡], Florence Bultelle[‡], Pierre Magal[¶], Glenn Webb[‖], and Frank Le Foll[‡2]

From the [‡]Laboratory of Ecotoxicology, University of Le Havre, 76058 Le Havre, France, [§]PRIMACEN, Cell Imaging Platform of Normandy, Inserm, Institute for Research and Innovation in Biomedicine (IRIB), University of Rouen, 76821 Mont-Saint-Aignan, France, [¶]UMR CNRS 5251 IMB and INRIA sud-ouest Anubis, University of Bordeaux, 33076 Bordeaux, France, and the [‖]Department of Mathematics, Vanderbilt University, Stevenson Center, Nashville, Tennessee 37240

Background: The P-glycoprotein is expressed in many human cancers, where it contributes to multi-drug resistance phenomenon.
Results: Both TnTs and microparticles contribute to the transfer of P-gp in MCF-7.
Conclusion: Our findings supply new mechanistic evidences for the extragenetic emergence of MDR in cancer cells.
Significance: Inhibition of both MPs and TnTs could be included in treatment strategies designed to overcome MDR.

Multi-drug resistance (MDR) is a phenomenon by which tumor cells exhibit resistance to a variety of chemically unrelated chemotherapeutic drugs. The classical form of multidrug resistance is connected to overexpression of membrane P-glycoprotein (P-gp), which acts as an energy dependent drug efflux pump. P-glycoprotein expression is known to be controlled by genetic and epigenetic mechanisms. Until now processes of P-gp gene up-regulation and resistant cell selection were considered sufficient to explain the emergence of MDR phenotype within a cell population. Recently, however, "non-genetic" acquisitions of MDR by cell-to-cell P-gp transfers have been pointed out. In the present study we show that intercellular transfers of functional P-gp occur by two different but complementary modalities through donor-recipient cells interactions in the absence of drug selection pressure. P-glycoprotein and drug efflux activity transfers were followed over 7 days by confocal microscopy and flow cytometry in drug-sensitive parental MCF-7 breast cancer cells co-cultured with P-gp overexpressing resistant variants. An early process of remote transfer was established based on the release and binding of P-gp-containing microparticles. Microparticle-mediated transfers were detected after only 4 h of incubation. We also identify an alternative mode of transfer by contact, consisting of cell-to-cell P-gp trafficking by tunneling nanotubes bridging neighboring cells. Our findings supply new mechanistic evidences for the extragenetic emergence of MDR in cancer cells and indicate that new treatment strategies designed to overcome MDR may include inhibition of both microparticles and Tunneling nanotube-mediated intercellular P-gp transfers.

P-glycoprotein (P-gp)[3] is a 170-kDa plasma membrane ATP binding cassette transporter encoded by the human *MDR1*/*ABCB1* gene that uses energy from ATP hydrolysis to actively efflux compounds from the cell (1–3). Physiological functions of P-gp rely on two remarkable molecular and cellular features. First, the substrate binding pocket of P-gp fits to a variety of chemically unrelated molecules, giving the protein the ability to transport a broad spectrum of substances encompassing lipids, peptides, and xenobiotics (4–6). Second, native expression of the *MDR1*/*ABCB1* gene is essentially restricted to tissue-blood epithelia in the brain, placenta, liver, testis, colon, and kidney in addition to isolated hematopoietic stem and immune cells (7–9). As a consequence, P-gp drains a variety of compounds across physiologic permeation barriers and lowers their concentrations in cell compartment.

In cancers developing from tissues possessing a natively high *MDR1*/*ABCB1* expression, the P-gp-mediated efflux of anticancer agents severely limits the efficacy of chemotherapy (10). In these tumors P-gp is, therefore, one of the major contributors to intrinsic multidrug resistance (MDR) (11). For other cancers, exposure to cytotoxics causes up-regulation of P-gp in neoplastic cells with a low basal level of the transporter and also induces a *de novo* expression of *MDR1*/*ABCB1* in non-expressing cells (12–14). Such cancers become secondarily multidrug resistant after a drug-induced switch-on of *MDR1*/*ABCB1* overexpression. Diverse mechanisms have been reported for contributing to *MDR1*/*ABCB1* up-regulation, including genomic instability, genetic induction of upstream or downstream *MDR1*/*ABCB1* promoters, in particular via the nuclear steroid and xenobiotic receptor, and epigenetic changes based on DNA methylation, histone acetylation, and microRNAome modifications (15–20). In all these pathways the pressure

* This work was supported by European Regional Development Fund as part of the Interreg IVA project Admin (Trans-Channel Advanced Microscopy network).
[S] This article contains supplemental Fig. 1 and supplemental videos 1 and 2.
[1] Recipient of a fellowship from the Conseil Regional de Haute-Normandie.
[2] To whom correspondence should be addressed. E-mail: frank.lefoll@univ-lehavre.fr.

[3] The abbreviations used are: P-gp, P-glycoprotein; MDR, multidrug resistance; MP, microparticle; WGA, agglutinin; TRITC, tetramethylrhodamine isothiocyanate; PE, phycoerythrin; FL, fluorescent light; HBSS, Hanks' balanced salt solution.

exerted by cytotoxics converges to a positive *MDR1*/*ABCB1* regulation followed by a selection and expansion of MDR cells in tumors (21, 22).

In 2005 Levchenko *et al.* (23) reported an additional mode of MDR acquisition in which intercellular transfers of P-gp arise between resistant P-gp overexpressing cells as donors and drug-sensitive cells as recipients. They showed that extragenetic acquisition of P-gp occurs both *in vitro* and *in vivo* and confers a MDR phenotype without *MDR1*/*ABCB1* expression in the recipient cells. From observations using co-cultures of adherent BE (2)-C cells with MDR sublines, the authors suggested that cell-to-cell P-gp transfers were contact-dependent. Similar transfers of P-gp through heterocellular contacts have been described between resistant mesothelial and sensitive epithelial ovarian cancer cells (24). Conversely, in a model of liquid tumor, an alternative mechanism of intercellular P-gp trafficking has been identified. In that case, MDR variants of the CCRF-CEM lymphoblastic leukemia cell line release P-gp-containing microparticles (MPs) that bind to drug-sensitive cells and transfer the protein and the efflux activity (25). As a whole, these studies indicate that a certain spreading of the MDR phenotype within cell populations originates in extragenetic transfers of P-gp. The phenomenon takes place in the absence of cytotoxic pressure, between different cell types, in various environments and, obviously, through distinct mechanisms. Nevertheless, the end effects of P-gp spreading may strongly depend on the mode of transfer. In a recent work we quantified some features of P-gp transfers in co-cultures of human breast cancer MCF-7 cells and used the data to feed a mathematical model, based on local P-gp exchanges, to estimate the rate and the consequences of P-gp exchanges in cell populations (26). However, the role of MPs as potential long distance P-gp vectors has not been considered. In the same way the preceding studies have been focused on MPs-mediated (25) or on contact-mediated P-gp transfers (23, 24) without considering a possible role of both pathways in the acquisition of MDR.

Herein, we identify intercellular membrane nanotubes, also termed cytonemes or tunneling nanotubes (TnTs), as short distance P-gp carriers between MCF-7 cells *in vitro*. Our results indicate that local P-gp transfers mediated by TnTs co-exist with remote P-gp transfers via MPs and are together responsible for the extragenetic emergence of MDR in a sensitive subpopulation co-cultured with resistant cells.

EXPERIMENTAL PROCEDURES

Cell Lines—The cell lines used in the present study were wild-type drug-sensitive human breast adenocarcinoma MCF-7, purchased at the American Type Culture Collection, and a multidrug resistant MCF-7/DOXO variant, kindly provided by Pr. J.-P. Marie (Hôtel Dieu, Paris, France). The cells were grown in RPMI 1640 medium supplemented with 5% heat-inactivated fetal bovine serum, 2 mM L-glutamine, and 1% antibiotic/antimycotic solution. Doxorubicin (1 μM) was added to the culture medium for the maintenance of the multidrug-resistant phenotype of MCF-7/doxo cells. Cultured cells were incubated at 37 °C under a water-saturated 95% air, 5% CO_2 atmosphere. Exposure of MCF-7/DOXO to the P-gp inhibitors verapamil or cyclosporine A dose-dependently abolished both resistance to doxorubicin and P-gp activity in MCF-7/doxo (27).

Confocal Microscopy—Live cell microscopy was used to image TnTs. Cells were labeled with 1 mg/ml Alexa Fluor® 594-conjugated wheat germ agglutinin (WGA, Invitrogen SARL, Cergy Pontoise, France) at 5 μg/ml for 10 min at 37 °C in the dark. WGA is a probe for detecting glycoconjugates that selectively binds to *N*-acetylglucosamine and *N*-acetylneuraminic acid residues of cell membranes.

Fixed cell confocal microscopy was performed by fixing cells in 3.7% formaldehyde in PBS for 5 min. Cells were then extensively washed in PBS, permeabilized with 0.1% Triton X-100 in PBS, and washed again in PBS. Cells were stained with a 50 μg/ml TRITC-conjugated phalloidin (Sigma) to label actin filaments.

For immunolocalization of P-gp, direct staining was performed with a phycoerythrin (PE)-conjugated UIC2 monoclonal antibody (mAb) solution (Beckman Coulter, Villepinte, France). Alternatively, an indirect immunodetection was carried out by using a non-conjugated UIC2 mAb solution (Beckman Coulter) revealed with a goat anti-mouse IgG2a γ_{2a} chain specific as secondary antibody (Beckman Coulter) at 1 μg/ml for 90 min. The UIC2 mAb reacts with an external epitope of P-gp.

For co-culture assays, 75% confluent-sensitive MCF-7 cells were loaded with 25 μM concentrations of the cell-permeant reactive fluorescent dye CellTracker Green (5-chloromethylfluorescein diacetate, Invitrogen) or CellTracker Violet (2,3,6,7-tetrahyfro-9-bromomethyl-1H,5H-quinolozino-(9,1-*gh*)-coumarin, Invitrogen) for 1 h at 37 °C in 25-cm^2 culture dishes. Cells were then washed twice with HBSS and covered with complete fresh culture medium. CellTracker is retained in living cells, inherited by daughter cells through several generations and not transferred to adjacent cells in a population. To prepare inserts for confocal microscopy, either CellTracker-loaded sensitive MCF-7 or MCF-7/DOXO or a carefully homogenized 50:50 mixture of ctgMCF-7:MCF-7/DOXO were plated at the desired density on glass coverslips placed in 35-mm culture dishes. Cells were allowed to adhere for 4 h. The culture medium was then completed, and cells were cultured for several hours or days according to assay. For P-gp immunodetection in mechanically dispersed co-cultures, mixtures of 50:50 ctgMCF-7:MCF-7/DOXO were directly grown in 35-mm dishes and mechanically dispersed just before plating on glass coverslips and staining with UIC2 mAb.

Slides were mounted in Mowiol (Calbiochem VWR International, Strasbourg, France). Imaging was performed using a Leica TCS SP2 upright confocal microscope (Leica Microsystems, Rueil-Malmaison, France). Post-acquisition image analysis was performed with LAS AF 1.8.2. and Imaris (Bitplane AG, Zurich Switzerland).

Extraction and Purification of Microparticles from Cell Cultures—Microparticles purification was conducted by using a two-step protocol modified from previously published methods (28, 29). Briefly, cells were grown to 75% confluency, and the medium was collected. Cells were then submitted to a mild trypsin digestion in calcium-free-medium to release microparticles loosely bound to their surface. This second incubation

medium was also collected. Pooled media were centrifuged at 2000 − *g* for 10 min to remove floating cells and debris. Cell-free supernatant was then transferred in 8 ultracentrifuge tubes and spun down at 100,000 × *g* for 1 h. The supernatant was removed, and the pellet was resuspended in HBSS. All pellets were pooled in one single ultracentrifuge tube and centrifuged at 100,000 × *g* for 1 h. The final pellet containing purified microparticles was either resuspended in RPMI for treatment of cell cultures or lysed for protein extraction or labeled for cytometry analysis or microscopy imaging.

Protein Extraction and Western Blot Analysis—Cells or microparticles were lysed in 10 mM Tris-HCl buffer, pH 8.0, containing 0.1% Triton X-100, 0.15 mM KCl, 5 mM β-mercaptoethanol, 1.3 mM EDTA, and 2 μM aprotinin. Protein lysates were placed on ice for 30 min, vortexed every 5 min, and cleared by centrifugation at 3500 × *g* for 15 min at 4 °C. The supernatants were collected and frozen at −80 °C until analysis. Protein concentration in extracts was determined using the Bradford method. Aliquots (40 μg) of total proteins extracted from cultured MCF-7 cells were subjected to electrophoresis through an 8% SDS-polyacrylamide gel at a constant voltage of 90 V in running buffer (25 mM Tris-HCl, pH 8.3, 192 mM glycine, and 0.1% SDS). Proteins were then transferred to nitrocellulose membrane overnight at 120 mA in transfer buffer (25 mM Tris-HCl, pH 8.3, 150 mM glycine, and 5% v/v methanol). The nitrocellulose membrane was blocked with 5% BSA in Tris-buffered saline (20 mM Tris, pH 7.6, 137 mM NaCl) for 2 h. Immunostaining was carried out using a mouse monoclonal P-gp C219 antibody (2 μg/ml, Abcam, Cambridge, UK) and a secondary polyclonal rabbit anti-mouse IgG peroxidase-conjugated antibody (1/40,000, Sigma). The enhanced chemiluminescence (ECL) detection system (GE Healthcare) was used for visualization of the secondary antibody as described in the manufacturer's manual. The signals from the blots were scanned using the ImageMaster TotalLab Version 1.11 software (GE Healthcare).

Analysis of P-gp Expression and Activity by Flow Cytometry—Cultured or co-cultured cells were trypsin-resuspended and washed with HBSS before analysis. The fluorescent light (FL) was quantified using a Cell Lab Quanta SC MPL flow cytometer (Beckman Coulter) equipped with a 22-milliwatt 488-nm excitation laser. Voltage settings of photomultipliers were not modified throughout the experiments. Each analysis consisted of a record of 10,000 events, triggered on electronic volume as primary parameter according to a particle diameter exceeding 8 μm. For intercellular P-glycoprotein transfer studies, P-gp was labeled using the PE-conjugated UIC2 mAb, as for fluorescence microscopy. Red fluorescence was measured in FL2 channel (log scale) through a 575-nm band pass emission filter. More than 93.1 ± 0.4% (mean ± S.E.) of gated events exhibited a FL2 >1. To study P-gp activity, resuspended cells were loaded with 0.25 μM calcein acetoxymethyl ester (Invitrogen) in RPMI for 15 min at 37 °C in the dark. Green FL was quantified via the FL1 channel (log scale) through a 525-nm band pass filter. Controls of MCF-7, MCF-7/DOXO, and extemporaneous mixtures of 50:50 MCF-7: MCF-7/doxo were analyzed before co-cultures in all experiments.

Co-incubation in Tissue Culture Inserts—The parental drug-sensitive cell line MCF-7 was plated on the bottom of a 6-well culture dish. After cell attachment, tissue culture inserts with 0.4-μm pore size PET capillary membranes (Thincerts, Greiner bio-one, Courtaboeuf, France) were positioned onto the wells. The multidrug resistant MCF-7/DOXO variant was then plated on the membrane surface of the tissue culture inserts. Cells were co-incubated for 6 days. After each day, cells were trypsin-resuspended and mixed together before analysis by flow cytometry.

RT-PCR—Total RNA was extracted from either separately cultured MCF-7 and MCF-7/DOXO cells or MCF-7 after a 6-day co-incubation with MCF-7/DOXO in tissue culture inserts. The extractions were performed using the RNeasy mini kit (Qiagen, Courtaboeuf, France) according to the manufacturer's recommendations. After genomic DNA removal by DNase digestion (Turbo DNA free kit, Applied Biosystems, Courtaboeuf, France), total RNA (1 μg) was reverse-transcribed with oligodT (Promega, Charbonnières, France) using the Superscript III First-Strand Synthesis SuperMix (Invitrogen). PCR analysis was performed with a MasterCycler apparatus (Eppendorf, Le Pecq, France) from 2 μl of cDNA using both ABCB1 primers, *i.e.* hABCB1-F (5′-CTCCGATACATGGTTTTCCG-3′), hABCB1-R (5′-CTCATGAGTTTATGTGCCACC-3′), and β-actin primers, *i.e.* h-actin-F (5′-GATGATGATATCGCCGCGCT-3′) and h-actin-R (5′-CTTCTCGCGGTTGGCCTTGG-3′). After an initial denaturation step at 94 °C for 2 min, 35 cycles were performed including a denaturation step at 94 °C for 30 s, annealing at 55 °C for 30 s, and extension at 72 °C for 30 s. The final extension step was continued for 5 min. β-Actin amplification was used as a qualitative control. DNA was omitted in non-template control. The absence of genomic DNA traces in RNA samples was checked by performing amplification from RNA without previous reverse transcription. PCR products were analyzed on a 1% agarose gel and visualized by SYBR staining (SYBR Safe DNA gel stain, Invitrogen). Amplicon length was evaluated using a standard molecular weight marker (100 bp DNA ladder, Promega).

Statistical Analysis—All quantitative data were expressed as the means ± S.E. Statistical analysis was performed by using SigmaPlot 11 (Systat Software Inc., Chicago, IL). A Shapiro-Wilk normality test, with a $p = 0.05$ rejection value, was used to test normal distribution of data before further analysis. All pairwise multiple comparisons were performed by one way analysis of variance followed by Holm-Sidak post hoc tests for data with normal distribution or by Kruskal-Wallis analysis of variance on ranks followed by Tukey post hoc tests in the case of failed normality test. Paired comparisons were performed by Student's *t* tests or by Mann-Whitney rank sum tests in the case of unequal variance or failed normality test. Statistical significance was accepted for $p < 0.05$ (*), $p < 0.01$ (**), or $p < 0.001$ (***).

RESULTS

Transfers of P-gp in Co-cultures—As in a previous work (26), to study P-gp transfers, drug-sensitive parental human breast cancer MCF-7 cells were mixed and co-cultured with an equivalent amount of multidrug-resistant P-gp overexpressing MCF-7 variants, selected for their resistance toward doxorubicin (MCF-7/Doxo). Surface P-gp expression was daily imaged

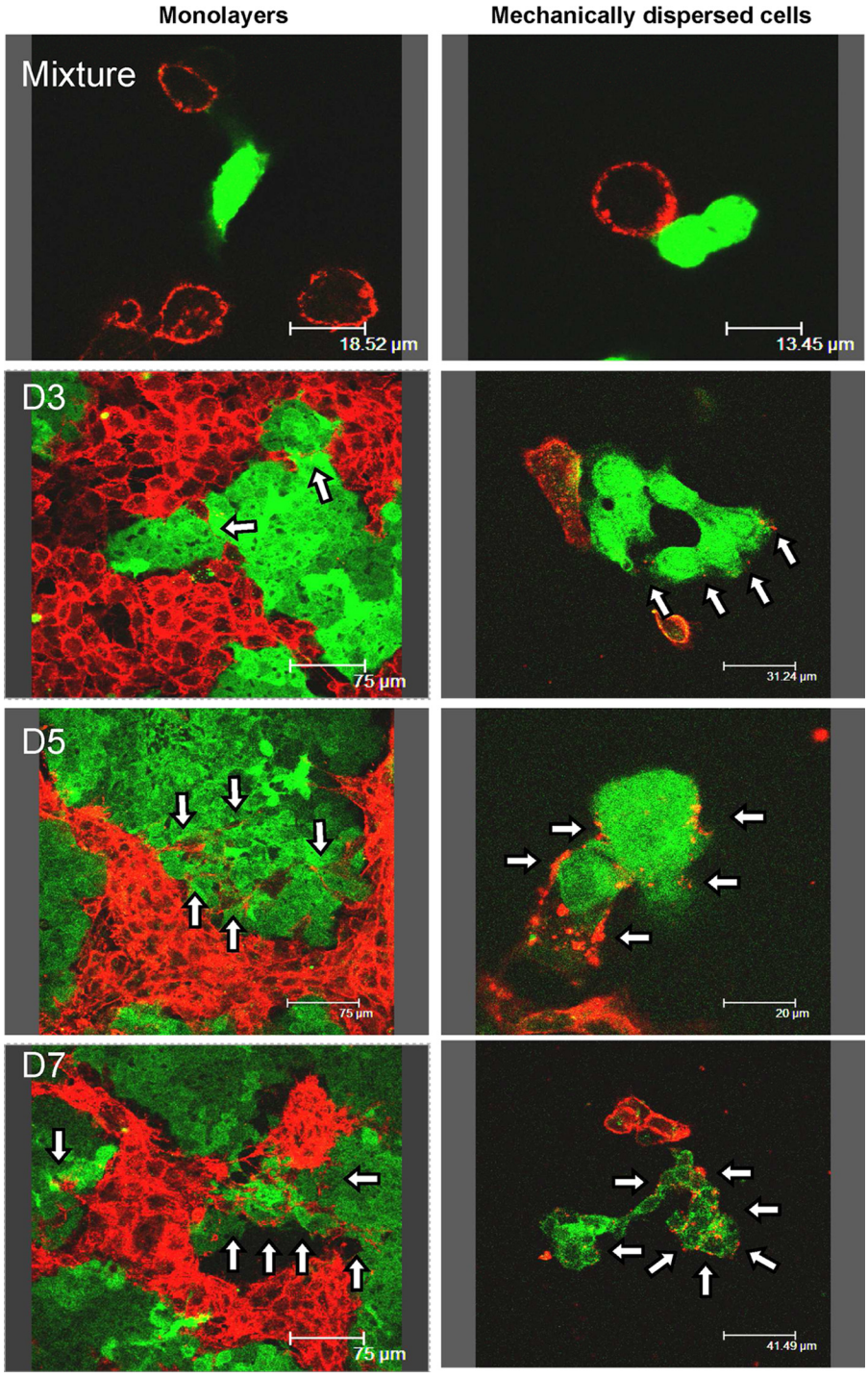

FIGURE 1. **Direct immunodetection of P-gp transfers in co-cultures of sensitive (MCF-7) and resistant (MCF-7/Doxo) variants of the human breast cancer cell line.** Before co-culture, MCF-7 were tagged with the persistent fluorescent probe CellTracker Green (ctgMCF-7). Mixtures of 50:50 ctgMCF-7:MCF-7/Doxo were co-cultured on glass coverslips during periods varying from 0 to 7 days (D0-D7). P-gp was immunodetected with phycoerythrin-conjugated (*PE*)-UIC2 mAb (*red fluorescence*) by confocal laser scanning microscopy in non-dispersed (*left column*) or mechanically dissociated cells (*right column*). Note that green fluorescence progressively fades because of dilution within daughter cells throughout mitoses. From D3 to D7, sensitive ctgMCF-7 show an increasing P-gp-specific red membrane staining (*arrows*), restricted to the plasma membrane, in non-dispersed as well as in dissociated cells.

by confocal microscopy after immunostaining with a phycoerythrin-conjugated UIC-2 monoclonal antibody directed against an extracellular epitope of P-gp (PE-UIC2 mAb). To be easily identified in co-cultures, the sensitive MCF-7 were tagged before seeding with the vital fluorescent tracer CellTracker Green (and, therefore, called ctgMCF-7). CtgMCF-7 and daughter ctgMCF-7 with inherited tracer can be easily identified in the co-cultures over several days. As shown in Fig. 1, *left*, after 3 days of co-culture, a progressive P-gp-immunostaining appeared at the membrane of ctgMCF-7. The staining gradually intensified from day 3 to day 7 and also penetrated from boundary cells to cells lying deeper in islets. P-gp immunofluorescence was clustered in small isolated bright spots in the early stages and then appeared more uniformly distributed

around ctgMCF-7 in older co-cultures. To make sure that what we interpreted as P-gp acquisition by ctgMCF-7 cells was not due to MCF-7/Doxo membrane expansions within ctgMCF-7 islets, experiments were repeated on cells mechanically dispersed just before imaging. Again, in these conditions a clear-cut P-gp staining restricted to plasma membrane was observed in isolated ctgMCF-7 (Fig. 1, *right*).

Acquisition of P-gp and Efflux Activity by Sensitive MCF-7—Co-culture experiments have been used to follow cell membrane P-gp contents over time, from day 0 to day 6, after staining with PE-UIC mAb and analysis by flow cytometry (Fig. 2). In Fig. 2*B*, a time-dependent shift of the peak corresponding to MCF-7 (in region R1) to the right, toward the regions of high P-gp levels, was observed. R1 peak fluorescence quantification showed a significant increase of FL2, from 3.60 ± 0.53 at day 0 to 17.90 ± 4.56 at day 5 of co-culture (Fig. 2*C*, mean ± S.E., n = 3–10, arbitrary fluorescence units).

To investigate whether P-gp transfers modify multidrug resistance activity of cell populations, the ability of co-cultures to efflux the P-gp fluorescent substrate calcein AM was followed over time. As shown in Fig. 3*A*, fluorescence accumulated in cells as an inverse function of P-gp activity, giving the possibility to separate fluorescent-sensitive MCF-7 from non-fluorescent resistant cells in a 50:50 extemporaneous mixture. In cells analyzed after co-culture, the peak of activity corresponding to initially sensitive cells (fluorescent region R2) progressively shifted to the left, toward regions of higher efflux activity. This observation is in good agreement with a progressive acquisition of P-gp. However, in addition to observations in analyses of cell membrane P-gp contents, the distribution in activity was characterized by the appearance of a third subpopulation displaying an intermediate efflux activity (in region R3). This new middle peak rose in amplitude with time. Concurrently, subpopulations of MCF-7 and, especially, of MCF-7/Doxo slightly decreased. At day 5 of co-culture, the cell count in R3 represented 23.72 ± 0.89% (mean ± S.E., n = 14, *black bars* in Fig. 4*D*) of the total cell number, whereas cells with this intermediate fluorescence level constituted only 11.29 ± 0.30% (n = 6) in the extemporaneous mixture of 50:50 MCF-7:MCF-7/Doxo at day 0.

Although time-progressive acquisition of P-gp and efflux activity by sensitive cells in the presence of resistant variants can occur through intercellular P-gp transfers, a *de novo* expression of P-gp by MCF-7 may alternatively originate from *MDR1*/*ABCB1* gene induction in response to various signaling factors secreted by co-cultures. To address this question, MCF-7 and MCF-7/Doxo were co-incubated in the same culture medium but separated by a permeable transwell membrane with a pore size of 0.4 μm. This filter porosity enables free diffusion of soluble paracrine factors and submicrometric particles but prohibits any cell-to-cell contact.

As in co-cultures, in the presence of the separating membrane, fluorescence of sensitive cells in region R2 gradually shifted toward the region of higher efflux activity. By contrast, the third population did not appear in the region R3 of intermediate efflux activity (Fig. 4*A*, *left*). From Fig. 4*C*, acquisition of efflux activity in region R2 for MCF-7 co-cultured in contact (n = 14, *black bars*) with MCF-7/Doxo did not significantly

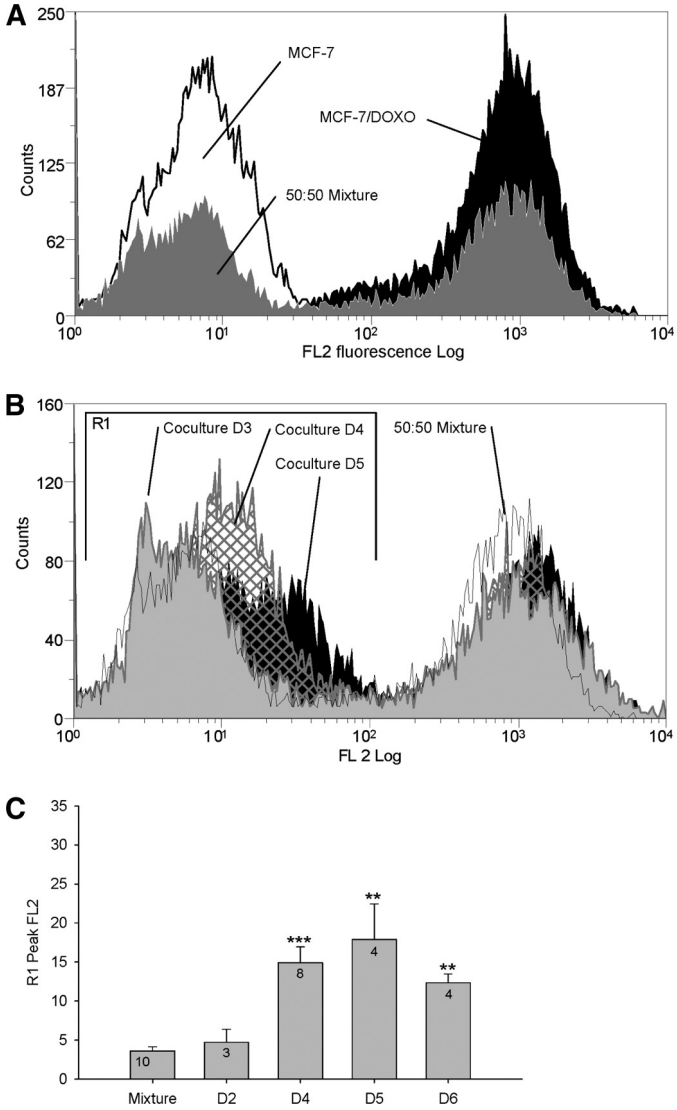

FIGURE 2. **Analysis by flow cytometry of P-gp transfers in co-cultures.** Membrane P-gp content was assessed by flow cytometry in the FL2 channel after direct immunolabeling with PE-UIC2. *A*, cell membrane P-gp content was quantified in parental MCF-7 (*open black histogram*), in resistant MCF-7/Doxo (*solid black histogram*), or in an extemporaneous mixture of 50:50 MCF-7:MCF-7/Doxo (*solid gray histogram*). *B*, membrane P-gp content was quantified in co-cultures. A 50:50 MCF-7:MCF-7/Doxo cell mixture was seeded on culture dishes at day 0 and trypsinized for increasing co-culture durations. P-gp distribution in an extemporaneous mixture of 50:50 MCF-7:MCF-7/Doxo was superimposed for comparison (*open black histogram*). Results obtained at days 3 (*solid gray histogram*), 4 (*hatched histogram*), and 5 (*solid black histogram*) show a progressive shift to the right of the peak initially corresponding to sensitive MCF-7 low P-gp expression. *C*, shown is a statistical comparison of the peak FL2 fluorescence in region R1 after different durations of co-culture (day D1 to D6), expressed as the mean ± S.E. of the replicate numbers indicated in the *bars*. Results significantly different from the mixture are indicated (*, $p < 0.05$; **, $p < 0.01$; ***, $p < 0.001$). The maximum P-gp transfer was observed at day 5.

differ from the gain of activity in MCF-7 co-incubated at distance (n = 7, *gray bars*) of resistant cells at days 4 and 5 ($p \geq 0.042$) but was significantly higher at day 6 ($p < 0.001$). The number of cells with intermediate efflux activity in region R3 was always rising and significantly higher in conditions of co-culture by comparison to transwell co-incubations at days 4, 5, and 6 (Fig. 4*D*). RT-PCR analysis of MCF-7 co-incubated at a distance from MCF-7/Doxo revealed that no significant pres-

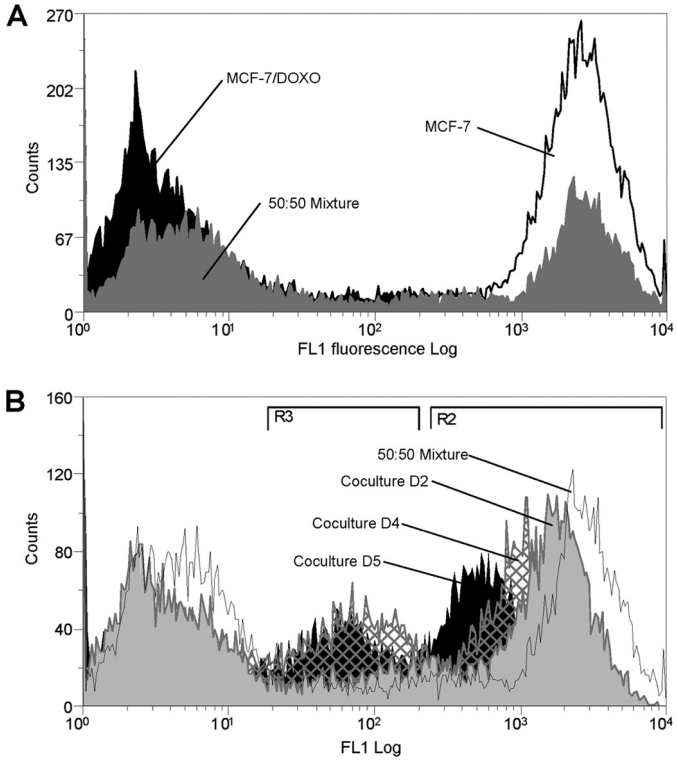

FIGURE 3. **Analysis by flow cytometry of P-gp activity transfers in co-cultures.** P-gp activity was measured as the ability to efflux the fluorescent P-gp substrate calceinAM. Intracellular fluorescence accumulation was quantified by flow cytometry in the FL1 channel. *A*, P-gp activity was measured in parental MCF-7 cells (*open black histogram*), in resistant MCF-7/Doxo cells (*solid black histogram*), or in an extemporaneous mixture of 50:50 MCF-7:MCF-7/Doxo (*solid gray histogram*). *B*, P-gp activity was measured in co-cultures. A 50:50 MCF-7:MCF-7/Doxo cell mixture was seeded on culture dishes at day 0 and trypsinized after increasing co-culture durations. P-gp activity distribution in an extemporaneous mixture of 50:50 MCF-7:MCF-7/Doxo was superimposed for comparison (*open black histogram*). Results obtained at days 2 (*solid gray histogram*), 4 (*hatched histogram*), and 5 (*solid black histogram*) show a gradual shift to the left of the peak initially corresponding to sensitive MCF-7 low activity. In addition, a third population exhibiting a middle range P-gp activity progressively appears with time.

ence of *MDR1*/*ABCB1* mRNA can be detected after 6 days of transwell experiment (Fig. 4*B*).

Taken together, these results confirm that MCF-7 acquired P-gp from MCF-7/Doxo without *MDR1*/*ABCB1* induction. In the absence of any cell-to-cell contact, P-gp transfers persisted but appeared lower than in co-cultures. This suggests the occurrence of different mechanisms of transfer. P-gp may be extragenetically acquired by sensitive cells through intercellular contacts with MCF-7/Doxo that could also, concurrently, release P-gp cargo particles able to spread smaller amount of P-gp through 0.4-μm pore size membranes. These points were investigated in the following experiments.

Microparticles as Remote Mechanism of Transfer—To isolate MPs from the culture medium of pre-confluent-resistant MCF-7, we used a two-step purification and centrifugation protocol (*cf.* "Experimental Procedures"). MPs detection was performed by flow cytometry. Because previous experiments evoked a diameter of less than 0.5 μm for MPs, a size below the detection limit of the electronic volume channel of our flow cytometer, we used the light scattering properties of particles to distinguish MPs from background noise. In the representative dot plots illustrated in Fig. 5*A*, the number of events associated to high side scatter signals was greater in the MP extract (*top middle panel*) than in control HBSS (*top left panel*). To increase MPs detection, membrane glycoconjugates in extracts were tagged by the lectin WGA conjugated to Alexa Fluor 594 before analysis in the FL1 channel. The huge number of detected events with both high fluorescence and scattering properties indicated the presence of MPs in MCF-7 (data not shown) and MCF-7/Doxo (*top right panel*) culture media.

P-gp content of MPs was examined by using immunolabeling with different monoclonal antibodies. By flow cytometry, P-gp was detected in the membrane of MPs purified from MCF-7/Doxo culture medium after direct staining with PE-UIC2 mAb and analysis in the FL2 channel (Fig. 5*A*, *bottom right panel*). In Western blots, P-gp was detected in total proteins extracted from MCF-7/Doxo MPs after indirect staining by using c219 as primary mAb (Fig. 5*B*).

Binding capabilities of microparticles to sensitive MCF-7 were explored by confocal imaging of living cells labeled with CellTracker Violet and incubated with MCF-7/Doxo MPs tagged by Alexa Fluor 594-conjugated WGA. Fig. 5*C* shows a progressive transfer of green fluorescence to the membrane of sensitive MCF-7, increasing with time from 30 s to 6 h.

MPs-mediated P-gp transfers were studied in experiments in which sensitive MCF-7 cells were exposed to P-gp-containing MPs purified from MCF-7/Doxo culture medium and analyzed by flow cytometry. Before analysis, repeatability in control distribution of surface fluorescence after PE-UIC2 direct immunolabeling (Fig. 6*A*) or of whole cell fluorescence after calceinAM incubation (Fig. 6*D*) was verified in sensitive MCF-7 from 5 independent cultures.

Incubation of sensitive MCF-7 with MCF-7/Doxo MPs transiently increased the relative cell surface expression of P-gp (Fig. 6*B*). A significant increase of surface P-gp was obtained as early as 4 h of incubation (Fig. 6*C*). Plasma membrane P-gp content peaked after 12 h of incubation, with a 4.42 $\pm$ 0.43-fold increase of fluorescence, and declined thereafter. Concomitantly, a significant efflux of calceinAM fluorescence was detected, also 2 h after the onset of exposure. Variations of efflux activity followed plasma membrane P-gp content, with a peak reached at 12 h, corresponding to a 0.57 $\pm$ 0.06-fold decrease of fluorescence and a subsequent fast return to the control fluorescence level (Fig. 6, *E* and *G*). To verify that the gain of efflux activity by parental MCF-7 was actually due to acquired P-gp activity, we used the archetypal non-competitive P-gp blocker PSC833, which fully inhibited P-gp-driven calcein efflux in MCF-7/Doxo (supplemental Fig. 1). After 6 h of exposure to MCF-7/Doxo MPs, efflux activity acquired by parental MCF-7 was completely abolished by 1 μM PSC833 (Fig. 6*F*).

Tunneling Nanotubes as Contact Mechanism of Transfer—In 2004, a new way of cell-to-cell communication based on tunneling nanotubes was reported (30). These labile plasma membrane cell bridges, with high length to diameter ratios, are known to appear *de novo* between cells in culture and to mediate intercellular transfers of organelles, various plasma membrane components, and cytoplasmic molecules (31). The presence of TnTs and their role in P-gp transfers were investigated in co-cultures of MCF-7:MCF-7/Doxo.

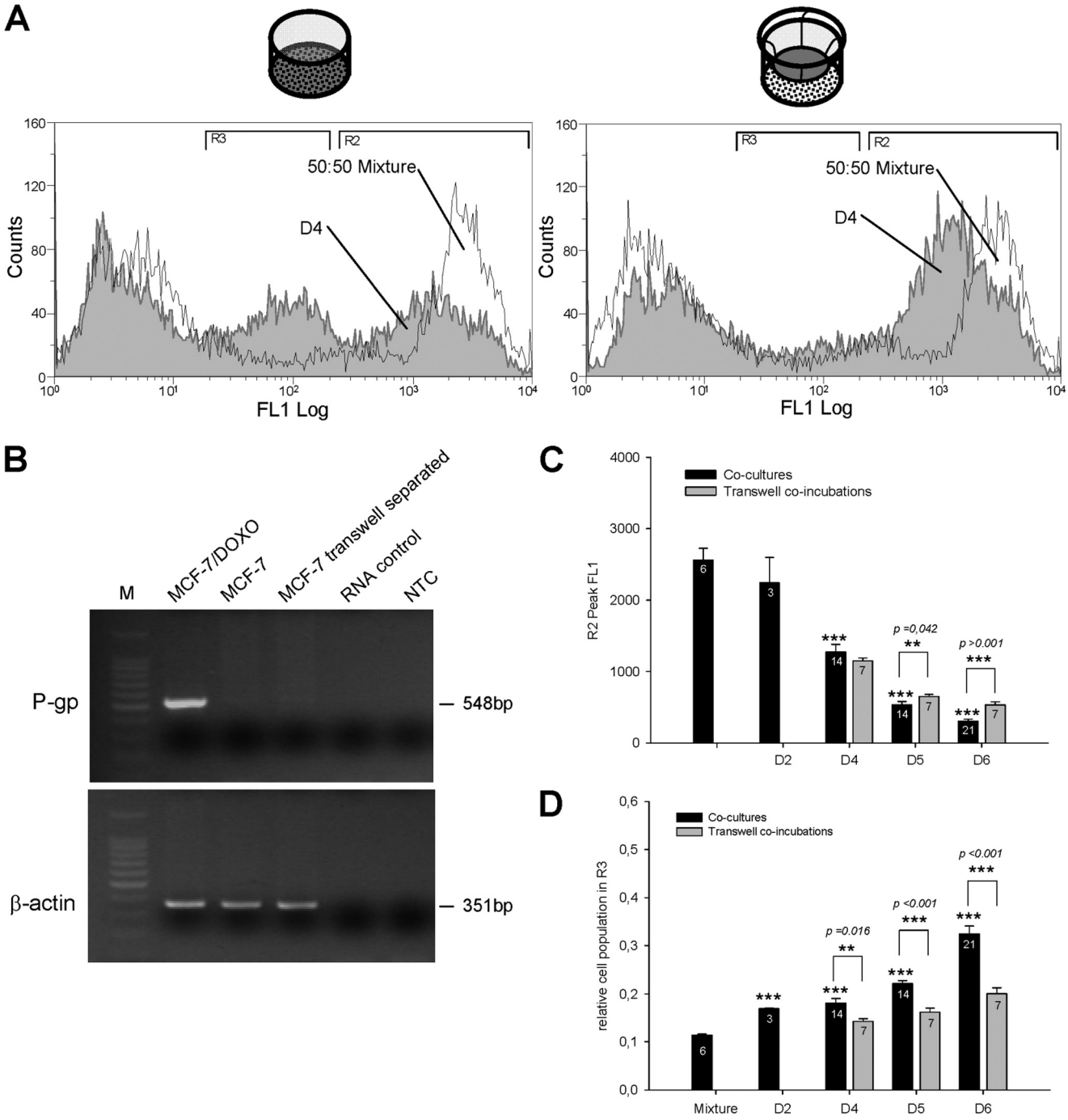

FIGURE 4. **Comparison of P-gp transcripts and activities in MCF-7 variants grown in open dish co-cultures or in membrane separated co-incubation chambers.** A mixture of 50:50 MCF-7:MCF-7/Doxo was co-cultured during 4 days in 6-well microplates or co-incubated separately on both sides of a 0.4-μm pore size PET capillary membrane of transwell tissue culture inserts. *A*, in cells co-cultured in an open dish, the P-gp activity distribution at day 4 was shifted toward left and displayed a population with an intermediate fluorescence level (*left*). In transwell-co-incubated cells at day 4, only the shift of activity was observed (*right*). *B*, shown are RT-PCR analyses in MCF-7 cells after co-incubation with MCF-7/Doxo through transwell tissue culture inserts. Total RNA was extracted from either separately cultured MCF-7/Doxo (*MCF-7/Doxo lane*) and MCF-7 cells (*MCF-7 lane*) or MCF-7 after a 6-day of co-incubation with MCF-7/Doxo in tissue culture inserts (*MCF-7 transwell separated lane*). RNA was then reverse-transcribed, and P gp cDNA was amplified using specific primers. A lack of genomic DNA in samples was checked by amplification from total RNA (*RNA control lane*). As a negative control, cDNA was omitted in non template control (*NTC lane*). β-Actin was amplified as a qualitative control. Amplicon length was evaluated using a standard molecular weight marker (*M*). No ABCB1 cDNA was detected in MCF-7 co-incubated with MCF-7/DOXO in tissue culture inserts. *C*, shown is a statistical comparison of the peak FL1 fluorescence in region R2 for cells analyzed from co-cultures (*black bars*) or from co-incubations in transwell tissue culture inserts (*gray bars*). Increase of efflux activity of the initially sensitive cell population was significant at day 4. No statistical differences appeared between co-cultured or transwell co-incubated cells at day 4. *D*, shown is a statistical comparison of the relative cell population in region R3 for cells analyzed from co-cultures (*black bars*) or from co-incubations in transwell tissue culture inserts (*gray bars*). The cell population in the intermediate activity region R3 was significantly less important in separated cells than co-cultured cells. All results are expressed as the mean $\pm$ S.E. of the replicate numbers indicated in the *bars*. Results significantly different from mixture are indicated *above the corresponding bars*, and differences between co-cultures and transwell co-incubations are indicated *above the brackets* (*, $p < 0.05$; **, $p < 0.01$; ***, $p < 0.001$).

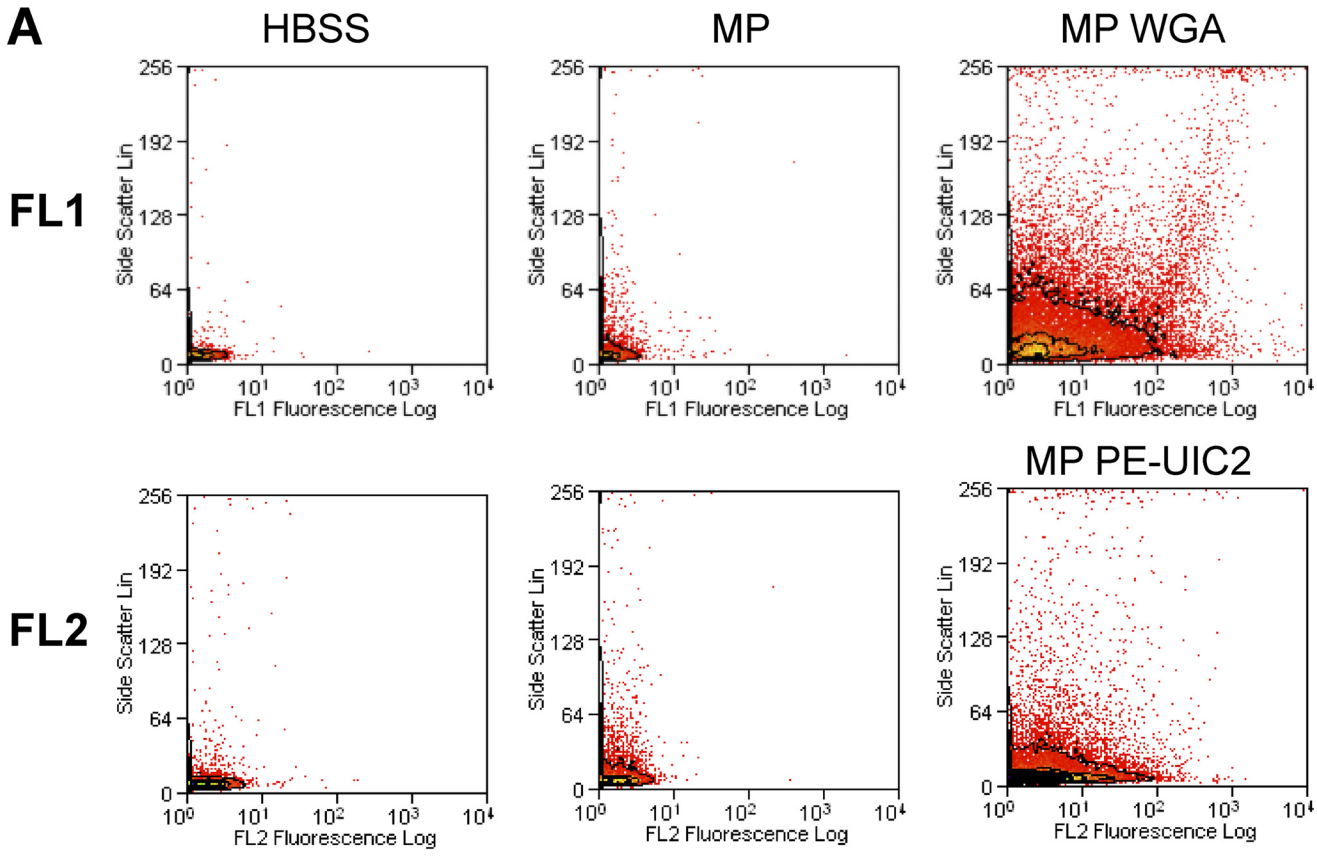

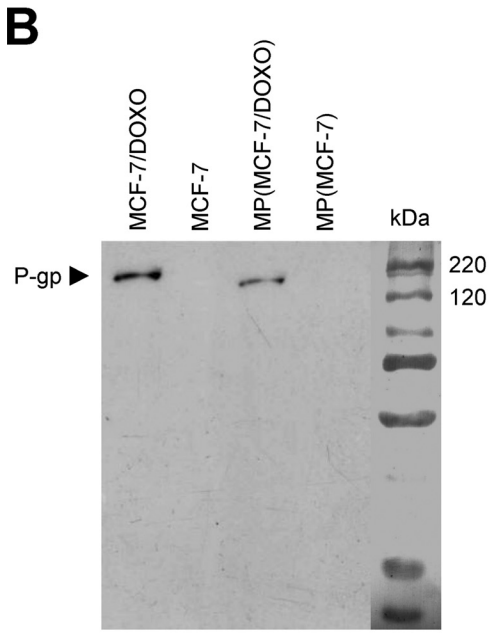

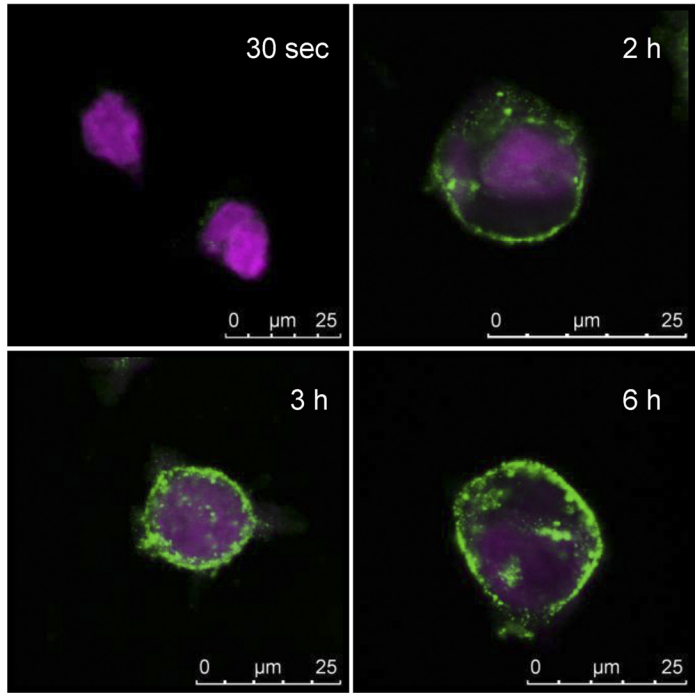

FIGURE 5. **Characterization of microparticles released by MCF-7/Doxo.** MPs were extracted and purified from MCF-7/Doxo cultures as described under "Experimental Procedures." *A*, MPs were detected in flow cytometry by their capability to diffract the laser light source and to give an increased side scatter signal (*middle dot plots*) by comparison to a sample of pure HBSS (*left dot plots*). Glycoconjugates in MP membranes were revealed with Alexa Fluor 594 conjugated-WGA and analyzed in the FL1 channel (*top right dot plots*). P-glycoprotein was detected in MPs by PE- UIC2 labeling in the FL2 channel (*bottom right dot plots*). *B*, total P-gp content of MPs was studied by Western blot using c219 as anti-P-gp primary mAb. P-gp was clearly detected in protein extracts from MCF-7/DOXO (*lane 1*) and from MPs extracted from MCF-7/DOXO cell cultures (*lane 3*) but not in extracts from MCF-7 (*lane 2*) and from MPs extracted from MCF-7 cell cultures. *C*, detection MP binding to MCF-7 cells is shown. CellTracker Violet-tagged MCF-7 cells were exposed to WGA-labeled MPs extracted from MCF-7/DOXO and imaged by confocal microscopy. Intensity of WGA labeling increased at the membrane of MCF-7 with time of incubation with MPs from 30 s to 6 h.

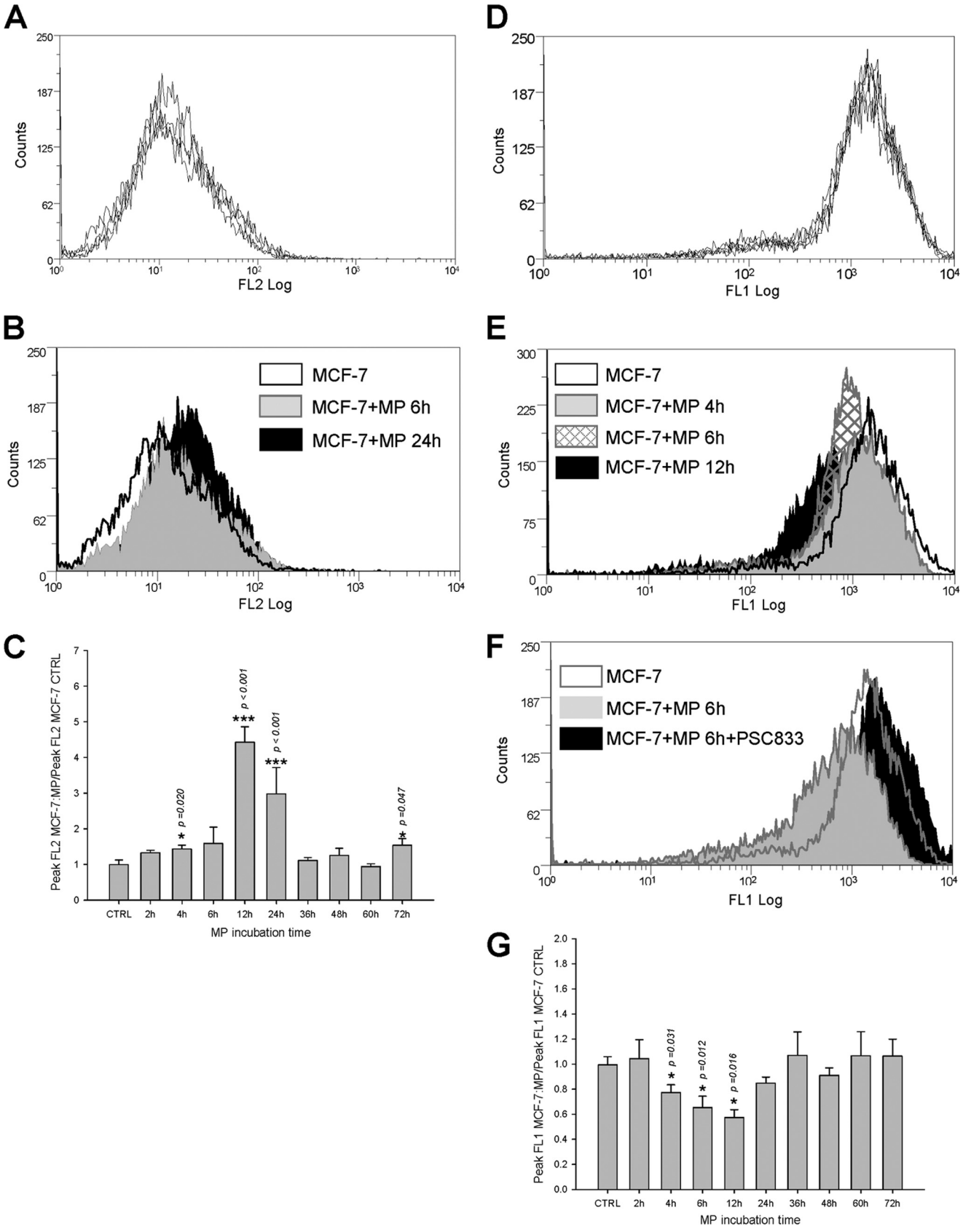

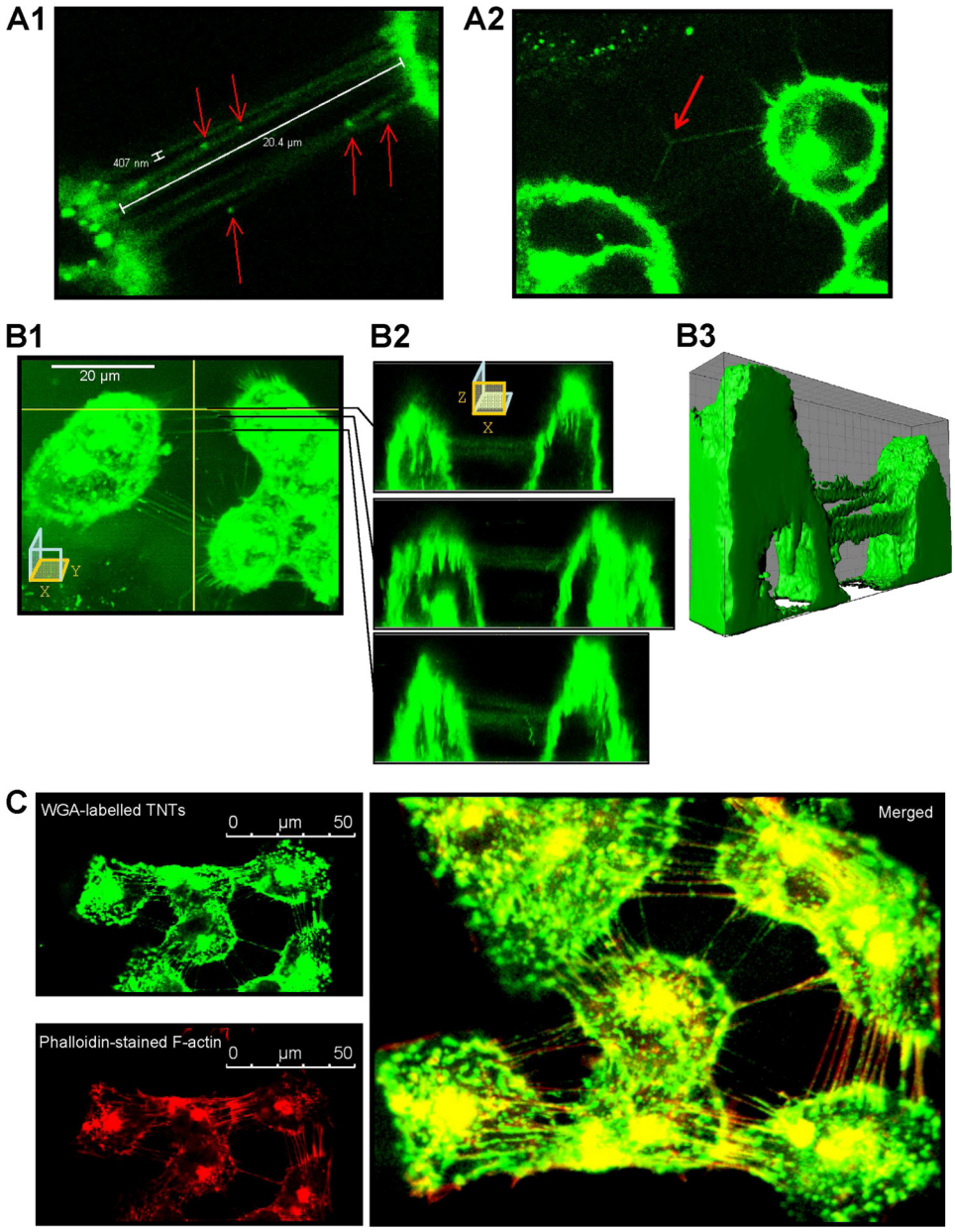

FIGURE 7. **Characterization of TnTs connecting MCF-7 cells in culture.** *A1*, Alexa Fluor 594 conjugated-WGA-stained MCF-7 cells were analyzed by live cell confocal microscopy. Cells are connected to surrounding cells by numerous ultrafine membrane extensions, namely TnTs, having a diameter inferior to 0.5 μm and a length of up to one cell diameter. WGA-stained organelles are seen at several points in TnTs (*arrows*). *A2*, branched TnTs were rarely observed. *B1–B2*, some TnTs were selected for *x-z* sections. TnTs did not contact the substrate. *B3*, shown is a three-dimensional reconstruction. *C*, fixed MCF-7 cells were stained with WGA (*top left image*) and TRITC-phalloidin (*bottom left image*). The merged image displays colocalization of WGA and TRITC-phalloidin staining, indicating that F-actin is a major component of TnTs (*right image*).

Confocal images recorded after WGA labeling of living MCF-7 in culture revealed structures connecting cells and fulfilling TnT size criteria (Fig. 7*A*), with a typical width of less than 0.5 μm and extensions over several cell diameters. Some TnTs exhibited punctual densities of fluorescence, which seems to correspond to the presence of subcellular organelles

FIGURE 6. **Transfers of P-gp and efflux activity to sensitive MCF-7 exposed to MPs extracted from MCF-7/DOXO.** *A*, repeatability of P-gp distributions in MCF-7, measured by flow cytometry after direct immunolabeling by PE-UIC2, is shown. Histograms from five independent cultures were superimposed. *B*, membrane P-gp content in MCF-7 (*open black histogram*) treated for 6 h (*solid gray histogram*) or for 24 h (*solid black histogram*) with MPs extracted from MCF-7/DOXO increased with time of exposure. *C*, relative increase of membrane P-gp content in MCF-7 cells treated with MPs extracted from MCF-7/DOXO was transient, significant after 4 h, and peaked after 12 h of exposure. Results are expressed as the mean ± S.E. of $n = 2$–10 replicates. *D*, repeatability of P-gp activity distributions in MCF-7, assessed by their ability to efflux intracellular fluorescence after loading with calceinAM, is shown. Histograms from five independent cultures are superimposed. *E*, P-gp activity in MCF-7 cells (*open black histogram*) treated for 4 h (*solid gray histogram*), 6 h (*hatched histogram*), or for 12 h (*solid black histogram*) with MPs extracted from MCF-7/DOXO increased with time. *F*, P-gp activity transferred to MCF-7 by a 6-h exposure to MPs extracted from MCF-7/DOXO was blocked by the specific P-gp antagonist PSC833 (20 μM). *G*, relative increase of P-gp activity, expressed as a drop of intracellular fluorescence, in MCF-7 treated with MPs extracted from MCF-7/DOXO was transient, significant after 4 h, and peaked after 12 h of exposure. Results are expressed as the mean ± S.E. of $n = 2$–10 replicates. Results significantly different from control are indicated (*, $p < 0.05$; **, $p < 0.01$; ***, $p < 0.001$).

(Fig. 7*A1*). Branched TnTs were rarely observed (Fig. 7*A2*). The main characteristic of TnTs is that they have no contact to the substratum and they hover in the extracellular medium (31). Selected (*x-z*) sections, obtained from confocal microscopy (Fig. 7, *B1* and *B2*), and three-dimensional reconstructions (Fig. 7*B3* and supplementary video) allowed identification of suspended TnTs interconnecting living MCF-7 cells. Co-localization of actin microfilaments, probed with tetramethylrhodamine isothiocyanate-phalloidin, and TnTs membranes, revealed by Alexa 594-WGA, were systematically observed in double staining experiments carried out in fixed MCF-7 (Fig. 7*C*). Confocal images presented herein correspond to 4-day-old cell cultures. TnTs were never observed in cells cultures having less than 3 days of incubation (data not shown).

The role of TnTs in intercellular P-gp transfers was explored by using live cell confocal microscopy and multiple staining co-cultures of 50:50 MCF-7:MCF-7/Doxo. In these experiments, parental-sensitive MCF-7 cells were tagged with CellTracker Violet as a vital fluorescent dye before seeding. After several days of co-culture, cells were incubated with Alexa 594-WGA to reveal TnTs membranes. In addition, P-gp was immunodetected by using UIC2 as the primary mAb. As shown by the representative merged images presented in Fig. 8, co-localization of the three dyes were found on many slides obtained at the third and fourth days of co-culture. P-gp-containing membrane bridges were frequently observed between MCF-7/Doxo and parental non-P-gp-expressing MCF-7. The anti-P-gp immunostaining always extended over the whole length of the TnTs. Nevertheless, in some sections of TnTs, an intense immunoreactivity appeared as aggregated strings. On many CellTracker Violet-identified parental MCF-7, P-gp was localized at the implantation point of TnTs and also on adjacent areas of the cell membrane, with an immunostaining intensity vanishing according to the distance.

DISCUSSION

In this work we give evidence for the existence of concurrent pathways in the transfer of functional P-gp from drug-resistant to drug-sensitive cancer cells. Previous studies have proposed that cell-to-cell P-gp transfers involved either cell contacts between adherent cells (23, 24) or were mediated by membrane microparticle release in liquid tumors (25). For the first time we establish that both cell-derived microparticles and membrane nanotubes carrying P-gp between neighboring cells contribute to the transfer in MCF-7 cell lines.

From our experiments, spontaneous induction of the *MDR1*/*ABCB1* gene leading to expression of P-gp was never observed in pure parental MCF-7 cultured in the absence of cytotoxics. Herein, we report that a progressive membrane P-gp immunostaining associated to a calcein efflux activity was detected in these cells after 2–6 days of co-culture with their drug-resistant P-gp-overexpressing counterpart. This observation may thus correspond to P-gp acquisition by transfer from resistant donor cells to sensitive recipient ones, as described earlier (23–26). However, the presence of resistant MCF-7/Doxo in the culture dish constitutes a modification of the cell environment that could provoke an increase in gene transcription. In particular, secretion of soluble factors able to induce *MDR1*/*ABCB1* has to be considered. Co-incubation experiments involving parental MCF-7 physically separated from resistant MCF-7/Doxo by transwell membranes with 0.4 μm pores were designed to address this issue. In these conditions, our results indicate that sensitive MCF-7 again acquired P-gp without *MDR1*/*ABCB1* induction, as revealed by the absence of P-gp transcript detection after MCF-7 RT-PCR analysis. These data lead us to conclude that the gain of P-gp by parental MCF-7 was dependent on cell-to-cell P-gp transfers that did not require proximity. The mechanism of transfer may thus involve diffusible intercellular cargos with, typically, a submicron size.

Interestingly, however, for long term 4–6-day experiments corresponding to the peak of membrane P-gp gain by MCF-7, we observed different quantities of efflux activity acquisition depending on whether sensitive and resistant cells were unconnectedly co-incubated or intimately co-cultured. Co-incubations led simply to a uniform shift of the sensitive cell population toward low levels of activity. By contrast, in the case of co-cultures allowing both remote and contact transfers, the acquisition of P-gp activity was characterized by a concurrent gain of low (R2 shift) and intermediate level (R3 increase) of calcein efflux.

The search for elements explaining additional gains of P-gp activity (typically in region R3), meeting the specific conditions of transfer with delay and contact has motivated confocal microscopy on living cells. Images revealed the occurrence of thin membrane bridges between neighboring cells. These high length-to-diameter ratio structures appeared to match the previously reported characteristics of tunneling nanotubes (for review, see Refs. 32 and 31), *i.e.* extending from cell to cell with no contact to substratum and filled with actin cytoskeleton. In several cell lines, TnTs have been shown to support cell-to-cell transfer of lipid anchored proteins (30). In this study, immunolabelings we obtained patently indicate that large membrane intrinsic glycoproteins such as P-gp can also travel between cells without leaving the lipid bilayer by diffusing laterally along the membrane of TnTs. Patchy or raft-like staining patterns likely corresponded to P-gp clusters, as this protein is known to alter local properties of lipid leaflets and to promote its own aggregation (33). The delay necessary to establish TnT connections as well as the cell proliferation needed for sufficient space-filling to bring MCF-7 cell bodies close enough may explain the latency separating the culture inoculation at day 0 and the detection of cells transferred in region R3 at day 3 in our experimental conditions. Further experiments are needed to determine whether TnT formation is based on outgrowth of filopodia protrusions under chemotactic guidance or rather on persistence of membrane bridges after separation of attached cells (31). Time-lapse imaging would also help to understand and to quantify time course and half-life of membrane bridge establishment in a dynamic environment governed by cell shape changes, migration, and growth.

As described for cell lines cultured in suspension (25), we found that resistant MCF-7 cells also spread P-gp-containing particles of micro- or submicrometric size in the culture medium. These microparticles can be detected after staining with the membrane specific WGA fluorescent dye. Incubation of sensitive MCF-7 with purified fluorescent MPs induced a

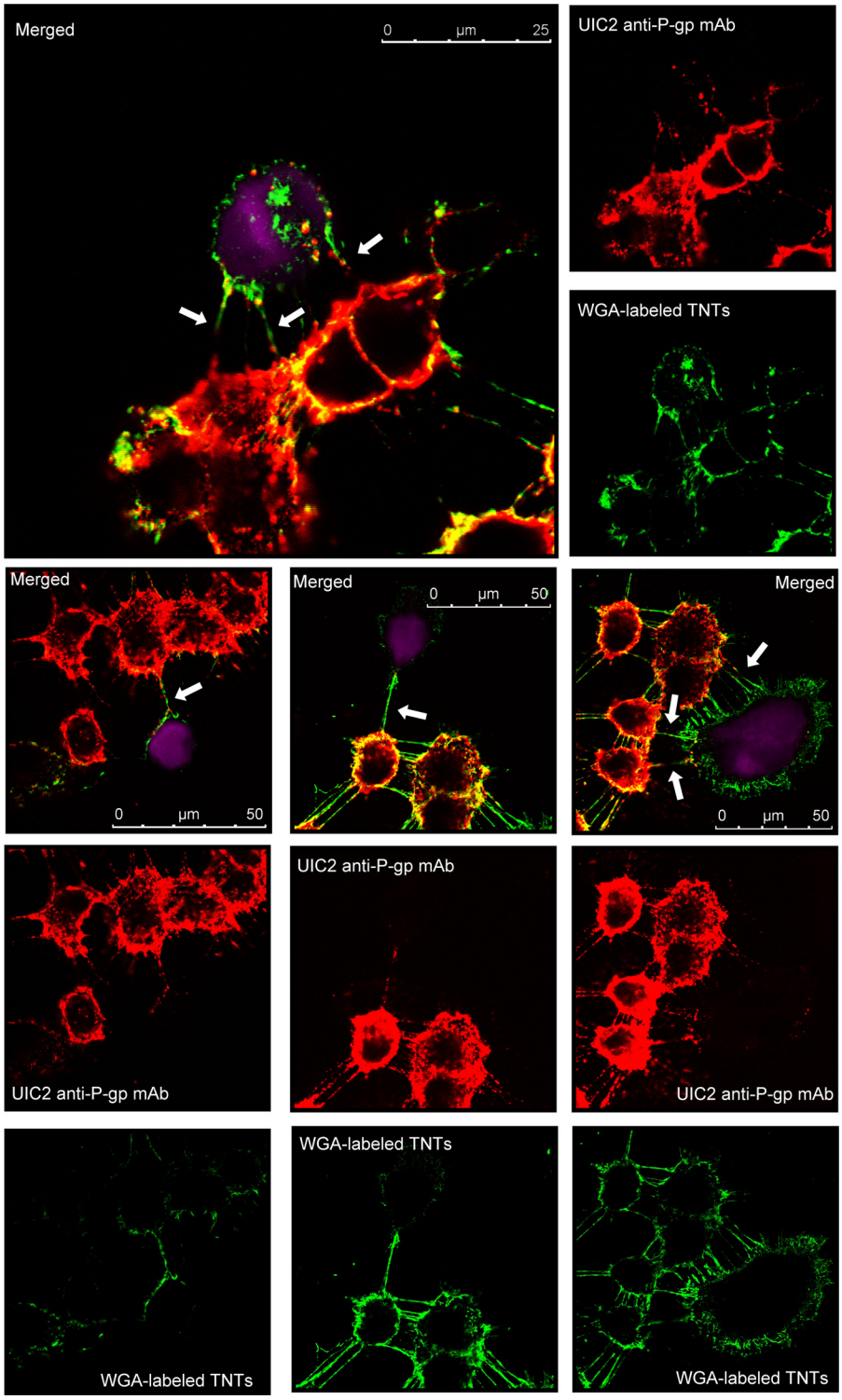

FIGURE 8. **Immunodetection of P-gp in TnTs connecting MCF-7/Doxo to MCF-7.** Sensitive MCF-7 were tagged with CellTracker Violet (ctvMCF-7, violet fluorescence), before co-culture. Mixtures of 50:50 ctvMCF-7:MCF-7/Doxo were co-cultured during 4 days on glass coverslips. P-gp was detected in fixed cells by using a non-conjugated UIC2 mAb as primary anti-P-gp mAb, revealed with a Texas Red-conjugated anti-mouse IgG2a γ2a (*red fluorescence*), and TnTs were labeled with WGA (*green fluorescence*). The figure presents different images of P-gp and TnTs localization within the co-cultures. Merged images present P-gp-containing TnTs connecting resistant MCF-7/Doxo to parental ctvMCF-7 cells (*arrows*).

transfer of fluorescence to the cell membrane in less than 2 h. This observation was interpreted as binding and fusion of MPs to cell membrane.

Exposure of sensitive cells to MPs purified from resistant MCF-7 induced a significant increase of membrane P-gp content and efflux activity detectable after a short interval of 4 h. This delay is compatible with the time range of MPs binding to cell membrane. This small time range is, however, likely not sufficient to provoke P-gp expression from *MDR1*/*ABCB1* gene induction, a process requiring 8–96 h in most cells (34–36).

Our findings are consistent with a past study reporting that a significant degree of resistance to doxorubicine can be transiently transferred to sensitive cells by polyethylene glycol-induced fusion with P-gp isolated from cell membrane of highly resistant cells (37).

All together, these results indicate that sensitive cells incorporate sufficient amounts of MPs-conveyed P-gp in correct functional orientation to exhibit an increased efflux activity. This amount could, however, be reduced (with a partition between P-gp correctly and incorrectly inserted in the membrane) by contrast to direct transfer mediated by TnTs. This assumption may provide an explanation for the differences observed in acquired activities according to the mode of transfer with, in both cases, similar gains in P-glycoprotein.

The exact nature of MPs detected and purified in this work was not determined (for a review on this concern, see Ref. 38); even so, a release of exosomes by MCF-7 has been shown (39). Excepting our study and the article of Bebawy *et al.* (25), P-gp was not previously identified in the proteome analysis of exosomes (40). However, another ABC transporter, the MRP2 protein, has been found in exosomes isolated from ovarian carcinoma cells (41).

The time-dependence study of MP-mediated P-gp transfers without MP renewal in the culture medium gave bell-shaped kinetics, with gains of protein and activity peaking after 12 h of incubation and dropping thereafter to control levels. This transient transfer capability of purified MPs was probably linked to a combination of particle lability in the incubation medium and processes of internalization/degradation of membrane transferred P-gp by recipient cells. The time-course of P-gp and efflux activity decrease in MP-transferred MCF-7 is consistent with the half-life of 12 h estimated for this protein (42) and rapid losses of membrane P-gp and activity, within minutes to hours, recently reported (43, 44).

The findings described above reveal the occurrence of multiple routes for extragenetic MDR acquisition by cell lines. In addition to genetic and epigenetic *MDR1*/*ABCB1* regulations, intercellular trafficking of the resistance protein contributes to spread the phenotype among neighboring cells, pushing boundaries for gene expression beyond the cell limit. Further studies are needed to establish whether the cell interconnections by TnTs, the release of MPs, and the addressing of P-gp to the corresponding membrane systems are regulated processes. However, our study highly suggests that these expression pathways take place at different times and distance scales in the cell microenvironment.

Acknowledgment—We are indebted to Pr. Jean-Pierre Marie (Hôtel Dieu, Paris, France) for providing MCF-7/Doxo and PSC833.

REFERENCES

1. Juliano, R. L., and Ling, V. (1976) A surface glycoprotein modulating drug permeability in Chinese hamster ovary cell mutants. *Biochim. Biophys. Acta* **455,** 152–162
2. Pastan, I., and Gottesman, M. (1987) Multiple-drug resistance in human cancer. *N. Engl. J. Med.* **316,** 1388–1393
3. Ambudkar, S. V., Kimchi-Sarfaty, C., Sauna, Z. E., and Gottesman, M. M. (2003) P-glycoprotein. From genomics to mechanism. *Oncogene* **22,** 7468–7485
4. Seelig, A., and Landwojtowicz, E. (2000) Structure-activity relationship of P-glycoprotein substrates and modifiers. *Eur. J. Pharm. Sci.* **12,** 31–40
5. Rosenberg, M. F., Callaghan, R., Modok, S., Higgins, C. F., and Ford, R. C. (2005) Three-dimensional structure of P-glycoprotein. The transmembrane regions adopt an asymmetric configuration in the nucleotide-bound state. *J. Biol. Chem.* **280,** 2857–2862
6. Zhou, S. F. (2008) Structure, function, and regulation of P-glycoprotein and its clinical relevance in drug disposition. *Xenobiotica* **38,** 802–832
7. Klimecki, W. T., Futscher, B. W., Grogan, T. M., and Dalton, W. S. (1994) P-glycoprotein expression and function in circulating blood cells from normal volunteers. *Blood* **83,** 2451–2458
8. Leslie, E. M., Deeley, R. G., and Cole, S. P. (2005) Multidrug resistance proteins. Role of P-glycoprotein, MRP1, MRP2, and BCRP (ABCG2) in tissue defense. *Toxicol. Appl. Pharmacol.* **204,** 216–237
9. Mizutani, T., Masuda, M., Nakai, E., Furumiya, K., Togawa, H., Nakamura, Y., Kawai, Y., Nakahira, K., Shinkai, S., and Takahashi, K. (2008) Genuine functions of P-glycoprotein (ABCB1). *Curr. Drug Metab.* **9,** 167–174
10. Goldstein, L. J., Galski, H., Fojo, A., Willingham, M., Lai, S. L., Gazdar, A., Pirker, R., Green, A., Crist, W., and Brodeur, G. M. (1989) Expression of a multidrug resistance gene in human cancers. *J. Natl. Cancer Inst.* **81,** 116–124
11. Leighton, J. C., Jr., and Goldstein, L. J. (1995) P-glycoprotein in adult solid tumors. Expression and prognostic significance. *Hematol. Oncol. Clin. North Am.* **9,** 251–273
12. Choi, C. H., Kim, H. S., Rha, H. S., Jeong, J. H., Park, Y. H., Min, Y. D., Kee, K. H., and Lim, D. Y. (1999) Drug concentration-dependent expression of multidrug resistance-associated protein and P-glycoprotein in the doxorubicin-resistant acute myelogenous leukemia sublines. *Mol. Cells* **9,** 314–319
13. Nieth, C., and Lage, H. (2005) Induction of the ABC-transporters Mdr1/P-gp (Abcb1), mrpl (Abcc1), and bcrp (Abcg2) during establishment of multidrug resistance after exposure to mitoxantrone. *J. Chemother.* **17,** 215–223
14. Meesungnoen, J., Jay-Gerin, J. P., and Mankhetkorn, S. (2002) Relation between MDR1 mRNA levels, resistance factor, and the efficiency of P-glycoprotein-mediated efflux of pirarubicin in multidrug-resistant K562 sublines. *Can. J. Physiol. Pharmacol.* **80,** 1054–1063
15. Riordan, J. R., Deuchars, K., Kartner, N., Alon, N., Trent, J., and Ling, V. (1985) Amplification of P-glycoprotein genes in multidrug-resistant mammalian cell lines. *Nature* **316,** 817–819
16. Synold, T. W., Dussault, I., and Forman, B. M. (2001) The orphan nuclear receptor SXR coordinately regulates drug metabolism and efflux. *Nat. Med.* **7,** 584–590
17. Baker, E. K., Johnstone, R. W., Zalcberg, J. R., and El-Osta, A. (2005) Epigenetic changes to the MDR1 locus in response to chemotherapeutic drugs. *Oncogene* **24,** 8061–8075
18. Chekhun, V. F., Kulik, G. I., Yurchenko, O. V., Tryndyak, V. P., Todor, I. N., Luniv, L. S., Tregubova, N. A., Pryzimirska, T. V., Montgomery, B., Rusetskaya, N. V., and Pogribny, I. P. (2006) Role of DNA hypomethylation in the development of the resistance to doxorubicin in human MCF-7 breast adenocarcinoma cells. *Cancer Lett.* **231,** 87–93
19. Kovalchuk, O., Filkowski, J., Meservy, J., Ilnytskyy, Y., Tryndyak, V. P., Chekhun, V. F., and Pogribny, I. P. (2008) Involvement of microRNA-451 in resistance of the MCF-7 breast cancer cells to chemotherapeutic drug doxorubicin. *Mol. Cancer Ther.* **7,** 2152–2159
20. Reed, K., Hembruff, S. L., Laberge, M. L., Villeneuve, D. J., Côté, G. B., and Parissenti, A. M. (2008) Hypermethylation of the ABCB1 downstream gene promoter accompanies ABCB1 gene amplification and increased expression in docetaxel-resistant MCF-7 breast tumor cells. *Epigenetics* **3,** 270–280
21. Fojo, T. (2007) Multiple paths to a drug resistance phenotype. Mutations, translocations, deletions, and amplification of coding genes or promoter regions, epigenetic changes, and microRNAs. *Drug Resist. Updat.* **10,** 59–67
22. Callaghan, R., Crowley, E., Potter, S., and Kerr, I. D. (2008) P-glycoprotein. So many ways to turn it on. *J. Clin. Pharmacol.* **48,** 365–378
23. Levchenko, A., Mehta, B. M., Niu, X., Kang, G., Villafania, L., Way, D.,

Polycarpe, D., Sadelain, M., and Larson, S. M. (2005) Intercellular transfer of P-glycoprotein mediates acquired multidrug resistance in tumor cells. *Proc. Natl. Acad. Sci. U.S.A.* **102,** 1933–1938
24. Rafii, A., Mirshahi, P., Poupot, M., Faussat, A. M., Simon, A., Ducros, E., Mery, E., Couderc, B., Lis, R., Capdet, J., Bergalet, J., Querleu, D., Dagonnet, F., Fournié, J. J., Marie, J. P., Pujade-Lauraine, E., Favre, G., Soria, J., and Mirshahi, M. (2008) Oncologic trogocytosis of an original stromal cells induces chemoresistance of ovarian tumors. *PLoS One* **3,** e3894
25. Bebawy, M., Combes, V., Lee, E., Jaiswal, R., Gong, J., Bonhoure, A., and Grau, G. E. (2009) Membrane microparticles mediate transfer of P-glycoprotein to drug sensitive cancer cells. *Leukemia* **23,** 1643–1649
26. Pasquier, J., Magal, P., Boulangé-Lecomte, C., Webb, G., and Le Foll, F. (2011) Consequences of cell-to-cell P-glycoprotein transfer on acquired multidrug resistance in breast cancer. A cell population dynamics model. *Biol. Direct* **6,** 5
27. Marin, M., Poret, A., Maillet, G., Leboulenger, F., and Le Foll, F. (2005) Regulation of volume-sensitive Cl^- channels in multidrug-resistant MCF7 cells. *Biochem. Biophys. Res. Commun.* **334,** 1266–1278
28. Shedden, K., Xie, X. T., Chandaroy, P., Chang, Y. T., and Rosania, G. R. (2003) Expulsion of small molecules in vesicles shed by cancer cells. Association with gene expression and chemosensitivity profiles. *Cancer Res.* **63,** 4331–4337
29. Théry, C., Amigorena, S., Raposo, G., and Clayton, A. (2006) Isolation and characterization of exosomes from cell culture supernatants and biological fluids. *Curr. Protoc. Cell Biol.* **30,** 3.22.1–3.22.29
30. Rustom, A., Saffrich, R., Markovic, I., Walther, P., and Gerdes, H. H. (2004) Nanotubular highways for intercellular organelle transport. *Science* **303,** 1007–1010
31. Gurke, S., Barroso, J. F., and Gerdes, H. H. (2008) The art of cellular communication. Tunneling nanotubes bridge the divide. *Histochem Cell Biol.* **129,** 539–550
32. Gerdes, H. H., and Carvalho, R. N. (2008) Intercellular transfer mediated by tunneling nanotubes. *Curr. Opin. Cell Biol.* **20,** 470–475
33. Oleinikov, V. A., Fleury, F., Ianoul, A., Zaitsev, S., and Nabiev, I. (2006) P-glycoprotein effect on the properties of its natural lipid environment probed by Raman spectroscopy and Langmuir-Blodgett technique. *FEBS Lett.* **580,** 4953–4958
34. Demeule, M., Brossard, M., and Béliveau, R. (1999) Cisplatin induces renal expression of P-glycoprotein and canalicular multispecific organic anion transporter. *Am. J. Physiol.* **277,** F832–F840
35. Geick, A., Eichelbaum, M., and Burk, O. (2001) Nuclear receptor response elements mediate induction of intestinal MDR1 by rifampin. *J. Biol. Chem.* **276,** 14581–14587
36. Pajic, M., Bebawy, M., Hoskins, J. M., Roufogalis, B. D., and Rivory, L. P. (2004) Effect of short term morphine exposure on P-glycoprotein expression and activity in cancer cell lines. *Oncol. Rep.* **11,** 1091–1095
37. Belli, J. A., Zhang, Y., and Fritz, P. (1990) Transfer of adriamycin resistance by fusion of Mr 170,000 P-glycoprotein to the plasma membrane of sensitive cells. *Cancer Res.* **50,** 2191–2197
38. Théry, C., Ostrowski, M., and Segura, E. (2009) Membrane vesicles as conveyors of immune responses. *Nat. Rev. Immunol.* **9,** 581–593
39. Staubach, S., Razawi, H., and Hanisch, F. G. (2009) Proteomics of MUC1-containing lipid rafts from plasma membranes and exosomes of human breast carcinoma cells MCF-7. *Proteomics* **9,** 2820–2835
40. Simpson, R. J., Jensen, S. S., and Lim, J. W. (2008) Proteomic profiling of exosomes. Current perspectives. *Proteomics* **8,** 4083–4099
41. Safaei, R., Larson, B. J., Cheng, T. C., Gibson, M. A., Otani, S., Naerdemann, W., and Howell, S. B. (2005) Abnormal lysosomal trafficking and enhanced exosomal export of cisplatin in drug-resistant human ovarian carcinoma cells. *Mol. Cancer Ther.* **4,** 1595–1604
42. Gottesman, M. M., Hrycyna, C. A., Schoenlein, P. V., Germann, U. A., and Pastan, I. (1995) Genetic analysis of the multidrug transporter. *Annu. Rev. Genet.* **29,** 607–649
43. Hawkins, B. T., Sykes, D. B., and Miller, D. S. (2010) Rapid, reversible modulation of blood-brain barrier P-glycoprotein transport activity by vascular endothelial growth factor. *J. Neurosci.* **30,** 1417–1425
44. Hawkins, B. T., Rigor, R. R., and Miller, D. S. (2010) Rapid loss of blood-brain barrier P-glycoprotein activity through transporter internalization demonstrated using a novel *in situ* proteolysis protection assay. *J. Cereb. Blood Flow Metab.* **30,** 1593–1597